Cell Reports, Volume *32*

Supplemental Information

Actin R256 Mono-methylation Is a Conserved Post-translational Modification Involved in Transcription

Ashok Kumar, Yuan Zhong, Amelie Albrecht, Pau Biak Sang, Adrian Maples, Zhenan Liu, Vinesh Vinayachandran, Rohit Reja, Chia-Fang Lee, Ashutosh Kumar, Jiyuan Chen, Jing Xiao, Bongsoo Park, Jianjun Shen, Bin Liu, Maria D. Person, Kathleen M. Trybus, Kam Y.J. Zhang, B. Franklin Pugh, Kristine E. Kamm, Dianna M. Milewicz, Xuetong Shen, and Prabodh Kapoor

Supplemental Information

Supplementary Table S1: List of PTMs identified through mass spectrometry in yeast cytoplasmic and nuclear actin. Related to Figure 1.

Positi-on from N-ter.	Targe-t	Modific-ation	Classification	High-est PTM Scor-e	Highest Peptide Confide-nce	Sequence Motif	Cytop lasm-ic Actin	Nuclear Actin (INO80)
3	S	Phosph o	Post-translational	100	High	MDsEVAALV	–	+
28	R	Methyl	Post-translational	100	High	AGDDAPrAVF PSI	+	–
61	K	Methyl	Post-translational	100	High	GDEAQSkRGI LTL	+	+
61	K	Acetyl	Multiple	100	High	GDEAQSkRGI LTL	+	+
61	K	GlyGly	Other	100	High	GDEAQSkRGI LTL	+	–
62	R	Methyl	Post-translational	100	High	DEAQSKrGILT LR	+	–
84	K	Methyl	Post-translational	100	High	NWDDMEkIW HHTF	+	+
95	R	Methyl	Post-translational	100	High	TFYNELrVAPE EH	+	+
113	K	Acetyl	Multiple	100	High	EAPMNPkSNR EKM	+	+
113	K	Methyl	Post-translational	100	High	EAPMNPkSNR EKM	+	+
113	K	GlyGly	Other	100	High	EAPMNPkSNR EKM	+	+
177	R	Methyl	Post-translational	100	High	LPHAILrIDLAG R	–	+
191	K	GlyGly	Other	100	High	LTDYLMkILSE RG	+	+
206	R	Methyl	Post-translational	100	High	FSTTAErEIVR DI	+	+
215	K	Methyl	Post-translational	100	High	VRDIKEkLCYV AL	+	+
215	K	Dimeth yl	Post-translational	100	High	VRDIKEkLCYV AL	+	+
238	K	Methyl	Post-translational	100	High	QSSSIEkSYEL PD	–	+
254	R	Methyl	Post-translational	100	High	ITIGNErFRAP EA	+	+
256	R	Methyl	Post-translational	100	High	IGNERFrAPEA LF	–	+

284	K	GlyGly	Other	100	High	TYNSIMkCDVDVR	–	+
284	K	Dimethyl	Post-translational	100	High	TYNSIMkCDVDVR	+	+
290	R	Dimethyl	Post-translational	100	High	KCDVDVrKELYGN	–	+
290	R	Methyl	Post-translational	100	High	KCDVDVrKELYGN	+	–
291	K	GlyGly	Other	100	High	CDVDVRkELYGNI	+	–
291	K	Methyl	Post-translational	100	High	CDVDVRkELYGNI	–	+
312	R	Methyl	Post-translational	100	High	FPGIAErMQKEIT	+	+
315	K	Methyl	Post-translational	100	High	IAERMQkEITALA	–	+
326	K	Acetyl	Multiple	100	High	LAPSSMkVKIIAP	+	+
326	K	Methyl	Post-translational	100	High	LAPSSMkVKIIAP	–	+
326	K	GlyGly	Other	100	High	LAPSSMkVKIIAP	+	–
328	K	GlyGly	Other	100	High	PSSMKVkIIAPPE	+	+
328	K	Acetyl	Multiple	100	High	PSSMKVkIIAPPE	–	+
335	R	Methyl	Post-translational	100	High	IIAPPErKYSVWI	+	–
373	K	Methyl	Post-translational	100	High	PSIVHHkCF	+	+
373	K	GlyGly	Other	100	High	PSIVHHkCF	+	–

Table S1: Actin PTMs in cytoplasmic and nuclear actin. Table showing actin PTMs detected by mass spectrometry in yeast cytoplasmic and nuclear actin. Antibodies raised against actin PTMs listed above with the yellow background. Western blot analyses using these actin PTM antibodies are consistent with the mass spectrometry data (See Figure 1). Mutations of residues marked in red color correspond to the mutations of smooth muscle actin *ACTA2* leading to human vascular diseases (See Supplemental Figure S4).

Supplementary Table S2: Proteins Identified with highest peptide confidence after immunoprecipitation followed by Mass Spectrometry Analyses using actin R256me1 antibody in *Saccharomyces cerevisiae* (strain ATCC 204508 / S288c). Related to Figure 4.

ACT1	**Actin**
RPO21	**DNA-directed RNA polymerase II subunit RPB1**
RPB2	**DNA-directed RNA polymerase II subunit RPB2**
RPC40	**DNA-directed RNA polymerases I and III subunit RPAC1**
RPA190	**DNA-directed RNA polymerase I subunit RPA190**
RPA135	**DNA-directed RNA polymerase I subunit RPA135**
TAF5	**Transcription initiation factor TFIID subunit 5**
INO80	**Chromatin-remodeling ATPase INO80**
RSC8	Chromatin structure-remodeling complex protein RSC8
RSC30	Chromatin structure-remodeling complex protein RSC30
SWI5	Transcriptional factor SWI5
SIN3	Transcriptional regulatory protein SIN3
PUF3	mRNA-binding protein PUF3
SRO9	RNA-binding protein SRO9
gag-pol	Probable RNA-directed RNA polymerase virus L-BC
SAM1	S-adenosylmethionine synthase 1
DIG1	Down-regulator of invasive growth 1
PAN1	Actin cytoskeleton-regulatory complex protein PAN1
SUB2	ATP-dependent RNA helicase SUB2
XRN1	5'-3' exoribonuclease 1
DHH1	ATP-dependent RNA helicase DHH1
DBP5	ATP-dependent RNA helicase DBP5
MPH1	ATP-dependent DNA helicase MPH1
RAD52	soform 2 of DNA repair and recombination protein RAD52
RFA1	Replication factor A protein 1
RFA2	Replication factor A protein 2
MSH6	DNA mismatch repair protein MSH6
MSH2	DNA mismatch repair protein MSH2
TDA11	Topoisomerase I damage affected protein 11

MGM101	Mitochondrial genome maintenance protein M
RIM1	Single-stranded DNA-binding protein RIM1, mitochondrial
TY2B-OR1	Transposon Ty2-OR1 Gag-Pol polyprotein
TY1B-MR2	Transposon Ty1-MR2 Gag-Pol polyprotein
SSC1	Heat shock protein SSC1, mitochondrial
HSC82	ATP-dependent molecular chaperone HSC82
HSP82	ATP-dependent molecular chaperone HSP82
MCM3	DNA replication licensing factor MCM3
PDC2	Protein PDC2
CDC16	Anaphase-promoting complex subunit CDC16
YIL108W	Putative zinc metalloproteinase YIL108W
PAT1	DNA topoisomerase 2-associated protein PAT1
TOP1	DNA topoisomerase 1
NSR1	Nuclear localization sequence-binding protein
KAP123	Importin subunit beta-4
KAP95	Importin subunit beta-1
SXM1	Importin beta SMX1
SEC7	Protein transport protein SEC7
SEC31	Protein transport protein SEC31
NUM1	Nuclear migration protein NUM1
SEC2	Rab guanine nucleotide exchange factor SEC2
AKL1	Serine/threonine-protein kinase AKL1
NOC2	Nucleolar complex protein 2
NET1	Nucleolar protein NET1
NOP56	Nucleolar protein 56
NOP58	Nucleolar protein 58
CUE5	Ubiquitin-binding protein CUE5
RPN10	6S proteasome regulatory subunit RPN10
URA2	Protein URA2
CDC19	Pyruvate kinase 1
IKI3	Elongator complex protein 1

YEF3	Elongation factor 3A
RPG1	Eukaryotic translation initiation factor 3 subunit A
GCN1	eIF-2-alpha kinase activator
RPL3	60S ribosomal protein L3
NIP1	Eukaryotic translation initiation factor 3 subunit C
PRT1	Eukaryotic translation initiation factor 3 subunit B
RPS1B	40S ribosomal protein S1-B
RPL2B	60S ribosomal protein L2-B
RPL27A	60S ribosomal protein L27-A
RPL16B	60S ribosomal protein L16-B
IKI3	Elongator complex protein 1
RPS0B	40S ribosomal protein S0-B
RPS11B	40S ribosomal protein S11-B
TIF34	Eukaryotic translation initiation factor 3 subunit I
GCD6	Translation initiation factor eIF-2B subunit epsilon
RPS9B	40S ribosomal protein S9-B
HCR1	Eukaryotic translation initiation factor 3 subunit J
TIF35	Eukaryotic translation initiation factor 3 subunit
SRP54	Signal recognition particle subunit SRP54
RPL32	60S ribosomal protein L32
GCD7	Translation initiation factor eIF-2B subunit beta
VMA1	V-type proton ATPase catalytic subunit A
VMA2	V-type proton ATPase subunit B
ARO1	Pentafunctional AROM polypeptide
UGP1	UTP-glucose-1-phosphate uridylyltransferase
EDE1	EH domain-containing and endocytosis protein 1

Table S2: Immunoprecipitation followed by Mass spectrometry analyses using actin R256me1 antibodies. Table showing mass spectrometry results for protein IDs using actin R256me1 antibodies. Experiments were done in triplicates and the peptides with the highest confidence (100%) are presented in the table. Subunits of RNA polymerases and transcription regulators identified are marked in Yellow.

Supplementary Table S3: RNA-Seq analyses of actin R256C mutant of yeast. Related to Figure 5.

Gene Set Name	Size	NES	FDR q-val
Down regulated			
Mitotic sister chromatid segregation	103	-2.54	0
Mitotic sister chromatid cohesion	38	-2.46	0
Sister chromatid segregation	111	-2.37	0
Chromosome segregation	198	-2.34	0
DNA dependent DNA replication	122	-2.32	0
Mitotic nuclear division	214	-2.30	0
Double strand break repair	109	-2.24	3.25E-04
Microtubule based process	121	-2.22	2.85E-04
DNA conformation change	89	-2.22	2.53E-04
Microtubule cytoskeleton organization	110	-2.20	6.48E-04
Mitotic cell cycle	377	-2.18	5.89E-04
DNA duplex unwinding	30	-2.15	0.0013
Mitotic cell cycle process	365	-2.14	0.0012
Microtubule polymerization or depolymerization	37	-2.14	0.0011
Microtubule nucleation	18	-2.13	0.0013
Establishment of sister chromatid cohesion	17	-2.11	0.0014
Chromosome condensation	19	-2.11	0.0014
Mitotic cell cycle checkpoint	56	-2.10	0.0018
DNA packaging	57	-2.09	0.0021
DNA geometric change	31	-2.09	0.0022
DNA replication	165	-2.09	0.0021
Negative regulation of mitotic cell cycle	63	-2.04	0.0038
DNA strand elongation involved in DNA replication	34	-2.02	0.0043
Cell cycle checkpoint	84	-2.02	0.0041
DNA strand elongation	37	-2.02	0.0043
Protein refolding	17	-2.02	0.0042
Sister chromatid cohesion	49	-2.01	0.0042
Recombinational repair	67	-2.01	0.0043
Microtubule polymerization	31	-2.00	0.0043
Up regulated			
Translational elongation	97	2.85	0.0000
Carbohydrate transport	43	2.10	0.0107
Monosaccharide transport	24	2.06	0.0183

Table S3: Genes set enrichment analysis was conducted (GSEA) on RNA-Seq gene expression data of actin R256C mutant compared to WT yeast. Significantly altered GSEA hallmarks are given in the table.

Supplementary Table S4: Transcriptional profile of the ACTA2: R258C TAAD patient derived fibroblast after RNA-seq analysis. Fibroblast from the healthy volunteers was used as controls. Related to Figure 5 and Supplemental Figure S5.

down-regulated in MT; up-regulated in MT

Ingenuity Canonical Pathways	-log(p-val	Ratio	z-score	Molecules	Total Pathway Genes = Molecules/Ratio	Down-reg Genes	Down-reg/Total	Up-reg Genes	Up-reg/Total
Interferon Signaling	6.39E00	2.65E-01	-2.828	IFIT1, IFITM3, OAS1, MX1, IFI35,STAT2, IRF9, PSMB8, IFITM1	34	9	0.265	0	0.000
Hepatic Fibrosis / Hepatic Stellate Cell Activation	5.65E00	9.9E-02		CTGF, COL4A1, COL8A1, COL4A2, CCL5, COL15A1, PGF, MYL7, COL5A3, CCL2, TIMP1, TNFSF12, CD70, TNFSF9, IGFBP3, TGFB2, COL11A1, COL18A1, TNFRSF1B, MMP1	202	12	0.059	8	0.040
Death Receptor Signaling	4.11E00	1.2E-01	-0.905	HSPB3, TNFSF12, HSPB2, PARP10, PARP12, ACTG2, TNFRSF1B, ACTC1, PARP9, ACTA1, PARP14	92	9	0.098	2	0.022
Virus Entry via Endocytic Pathways	3.98E00	1.16E-01		DNM1, FYN, CD55, ITGA3, RRAS2, HLA-C, ITGA2, HLA-B, ACTG2, ACTC1, ACTA1	95	8	0.084	3	0.032
Eicosanoid Signaling	3.86E00	1.22E-01	-1.000	PTGIS, PLA2G16, PTGFR, AKR1C3, LTC4S, PLA2G4C, RARRES3, ALOX5AP, PTGS2, PTGER1	82	8	0.098	2	0.024
Agranulocyte Adhesion and Diapedesis	3.8E00	8.42E-02		CLDN11, MMP3, ITGA2, CCL5, CXCL6, MYL7, ITGA3, CCL2, EZR, CXCL14, PODXL, CCL26, ACTG2, ACTC1, ACTA1, MMP1	190	8	0.042	8	0.042
Caveolar-mediated Endocytosis Signaling	3.56E00	1.23E-01		FYN ,CD55, ITGA3, HLA-C, ITGA2, HLA-B, ACTG2, ACTC1, ACTA1	73	7	0.096	2	0.027
Role of Pattern Recognition Receptors in Recognition of Bacteria and Viruses	3.44E00	9.45E-02	-2.449	IFIH1, OAS1, IRF7, OAS2, IL17D, DDX58, CASP1, TGFB2, CCL5, EIF2AK2, OAS3, IL11	127	10	0.079	2	0.016
Aryl Hydrocarbon Receptor Signaling	3.43E00	8.9E-02		HSPB3, ALDH1B1, GSTM1, GSTM5, GSTM3, NQO2, HSPB2, CCND1, CYP1B1, GSTT1, GSTT2/GSTT2B, ALDH1A1, TGFB2	101	9	0.089	4	0.040
Cell Cycle: G2/M DNA Damage Checkpoint Regulation	3.28E00	1.43E-01	2.646	CDC25B, CKS1B, TOP2A, CCNB2, PLK1, AURKA, CCNB1	49	7	0.143	0	0.000

Figure S1

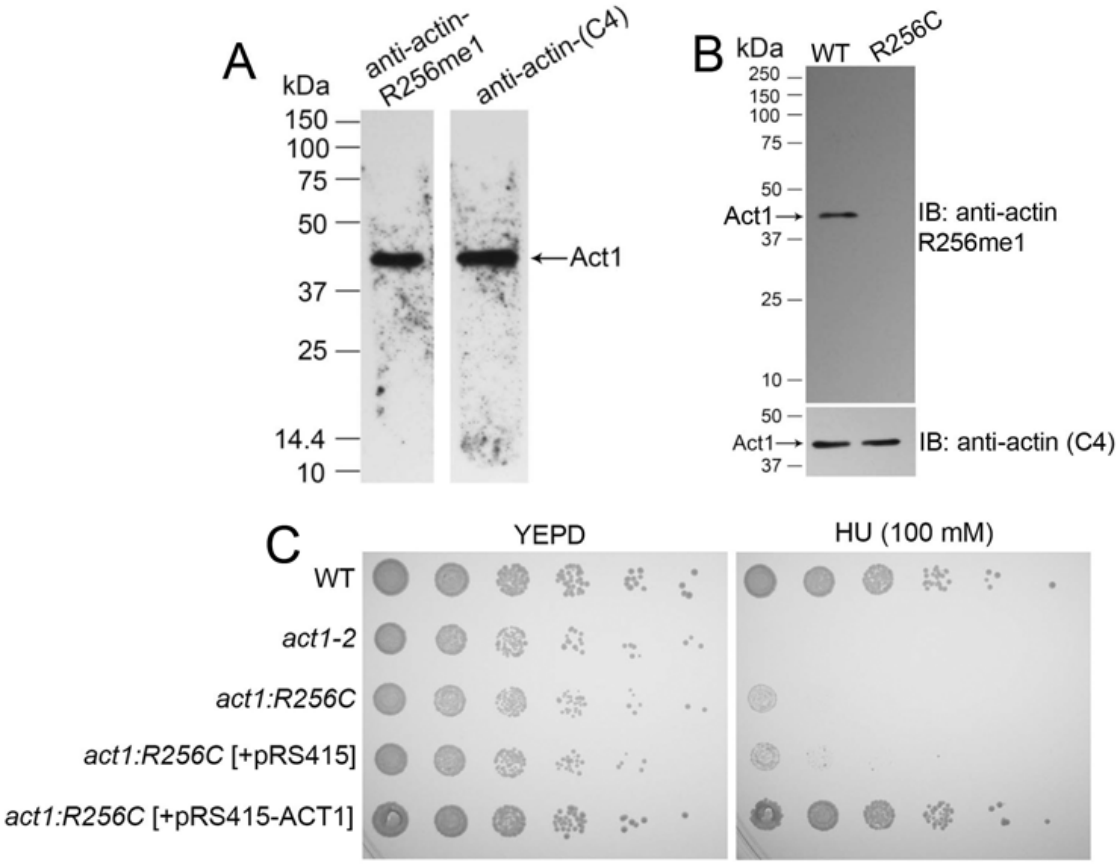

D

```
Drosophila  MCDEEVAALVVDNGSGMCKAGFAGDDAPRAVFPSIVGRPRHQGVMVGMGQKDSYVGDEAQ
Human       -MDDDIAALVVDNGSGMCKAGFAGDDAPRAVFPSIVGRPRHQGVMVGMGQKDSYVGDEAQ
Yeast       -MDSEVAALVIDNGSGMCKAGFAGDDAPRAVFPSIVGRPRHQGIMVGMGQKDSYVGDEAQ
                3                          28

Drosophila  SKRGILTLKYPIEHGIVTNWDDMEKIWHHTFYNELRVAPEEHPVLLTEAPLNPKANREKM
Human       SKRGILTLKYPIEHGIVTNWDDMEKIWHHTFYNELRVAPEEHPVLLTEAPLNPKANREKM
Yeast       SKRGILTLRYPIEHGIVTNWDDMEKIWHHTFYNELRVAPEEHPVLLTEAPMNPKSNREKM
            61-62                  84          95                  113

Drosophila  TQIMFETFNTPAMYVAIQAVLSLYASGRTTGIVLDSGDGVSHTVPIYEGYALPHAILRLD
Human       TQIMFETFNTPAMYVAIQAVLSLYASGRTTGIVMDSGDGVTHTVPIYEGYALPHAILRLD
Yeast       TQIMFETFNVPAFYVSIQAVLSLYSSGRTTGIVLDSGDGVTHVVPIYAGFSLPHAILRID
                                                                    177

Drosophila  LAGRDLTDYLMKILTERGYSFTTTAEREIVRDIKEKLCYVALDFEQEMATAASSSSLEKS
Human       LAGRDLTDYLMKILTERGYSFTTTAEREIVRDIKEKLCYVALDFEQEMATAASSSSLEKS
Yeast       LAGRDLTDYLMKILSERGYSFSTTAEREIVRDIKEKLCYVALDFEQEMQTAAQSSSIEKS
                        191             206     215                 238

Drosophila  YELPDGQVITIGNERFRCPEALFQPSFLGMEACGIHETTYNSIMKCDVDIRKDLYANTVL
Human       YELPDGQVITIGNERFRCPEALFQPSFLGMESCGIHETTFNSIMKCDVDIRKDLYANTVL
Yeast       YELPDGQVITIGNERFRAPEALFHPSVLGLESAGIDQTTYNSIMKCDVDVRKELYGNIVM
                        254 256                         284  290-291

Drosophila  SGGTTMYPGIADRMQKEITALAPSTMKIKIIAPPERKYSVWIGGSILASLSTFQQMWISK
Human       SGGTTMYPGIADRMQKEITALAPSTMKIKIIAPPERKYSVWIGGSILASLSTFQQMWISK
Yeast       SGGTTMFPGIAERMQKEITALAPSSMKVKIIAPPERKYSVWIGGSILASLTTFQQMWISK
                      312  315       326 328    335

Drosophila  QEYDESGPSIVHRKCF
Human       QEYDESGPSIVHRKCF
Yeast       QEYDESGPSIVHHKCF
                      373
```

Figure S1: Western blot analysis and rescue experiment of actin R256C mutant yeast strains, and sequence alignment of actin from different organisms. Related to Figure 1, Figure 2, and Figure 3. (A), Western blot analysis of the whole cell yeast extract after probing with actin R256me1 antibodies (left panel), the blot was stripped off and stained with and anti-actin (C4) antibodies (right panel). Actin R256me1 antibodies detects a single band at the molecular size of actin (~42 kDa), similar to anti-actin (C4) antibodies in the whole cell yeast extract. (B), Western blot analysis of the whole cell yeast extract from WT and R256C mutant strains after probing with actin R256me1 antibodies (upper panel), and anti-actin (C4) antibodies (lower panel). Actin R256me1 antibodies detects a single band at the molecular size of actin (~42 kDa), similar to anti-actin (C4) antibodies in the whole cell yeast extract from WT strains. However, actin R256me1 antibodies do not detects any band in the whole cell yeast extract from *act1:R256C* mutant strains. (C), Phenotypic analyses on YEPD and HU (100mM) plate at permissive temperature (30 °C), showing the recovery of growth of the actin R256C mutants in the presence of a plasmid expressing the wild type actin (pRS415-ACT1). (D), For amino acid sequence alignment ClustalW analyses of Yeast actin (Act1), Human β-actin, and *Drosophila melanogaster* actin isoform B was done. Amino acid numbered at the bottom of the sequences are the residues that are observed to be posttranslationally modified through mass spectrometry in the yeast nuclear actin (See Table S1). All of these residues except Serine-3 are found to be conserved from yeast to human.

Figure S2

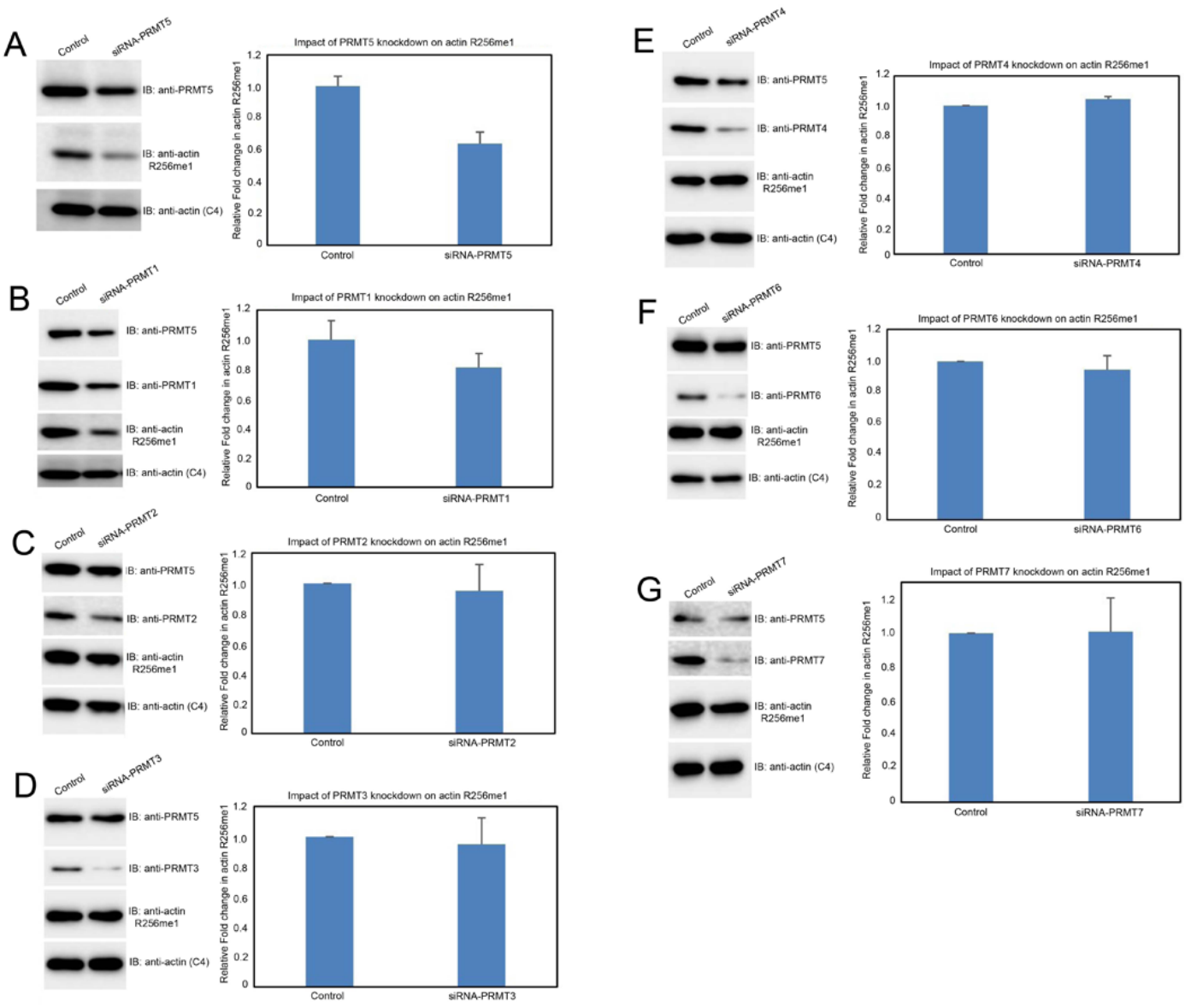

Figure S2: Knockdown of PRMTs show that PRMT5 is required for actin R256 methylation (R258 in human actin) in HEK293 cells. Related to Figure 3.

(A-G), Left panel; Western blot analyses of the whole cell extract of HEK293 cells transfected with siRNA against individual PRMTs as mentioned at the top, using antibodies indicated at the right. Right Panel; Graph shows the relative folds change in actin R256me1 level (R258 in human actins) after siRNA of individual PRMTs in HEK293 cells. Data presented is the mean of three independent experiments.

Figure S3

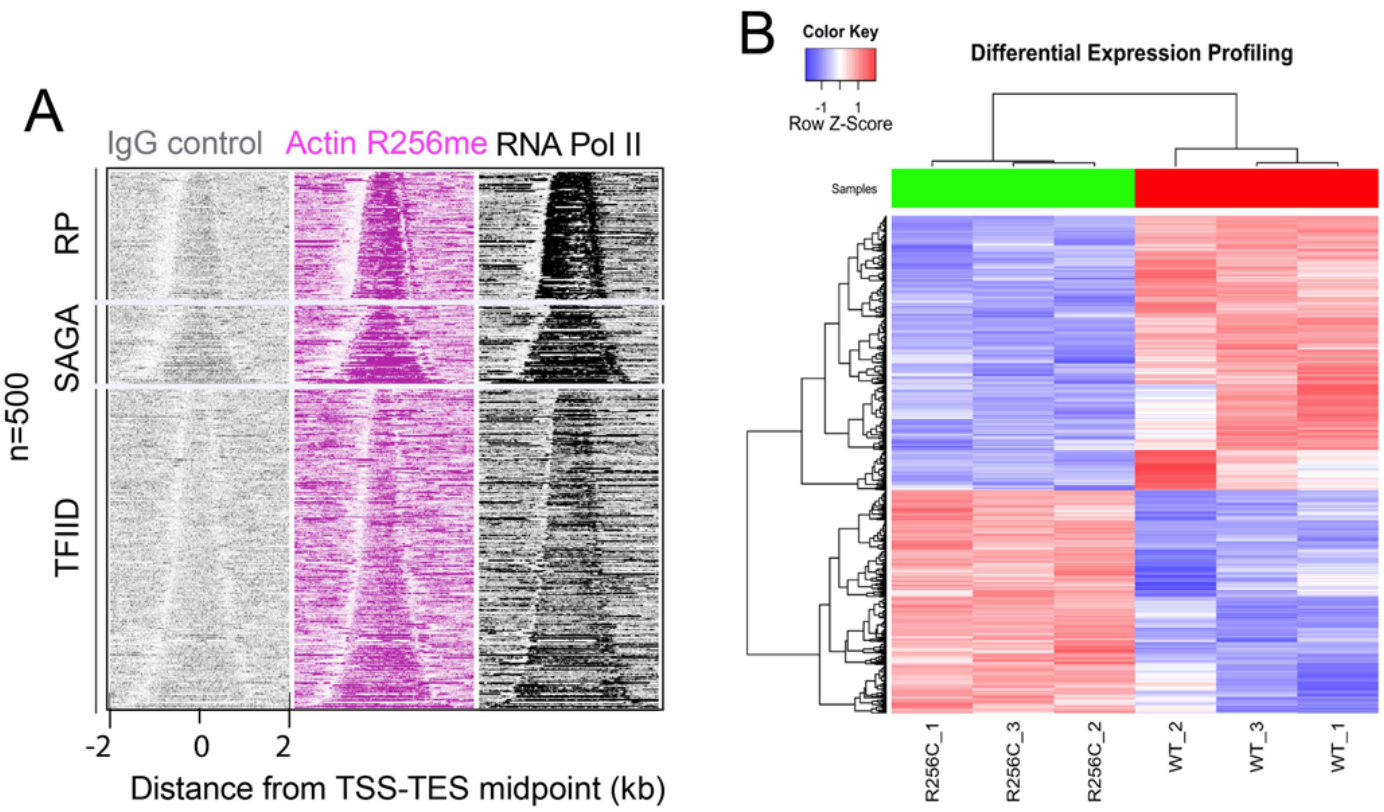

Figure S3: ChIP-exo analysis of yeast genome using actin R256me1 antibodies, and differential expression profiling of WT and actin R256C mutant yeast strains. Related to Figure 4, and Figure 5. (A), Bell plots showing shifted 5' tag ends for actin R256me, IgG control, and RNA polymerase II aligned by the midpoint of Transcription Start Site (TSS) and Transcription End Site (TES) of 500 significantly enriched genes, grouped into Ribosomal Protein (RP), SAGA, and TFIID genes sorted by gene length in each group. (B), A hierarchically clustered heatmap showing the expression patterns of the differentially expressed genes (fold change >=2) for the three biological replicates of WT and actin R256C mutant yeast strain. Red and blue color represents up- and down-regulated expression respectively. Color density indicating levels of fold change is displayed. Pearson distance correlation was calculated and Z-score is shown in the bar graph at the top. Complete hierarchical clustering was used for grouping.

Figure S4

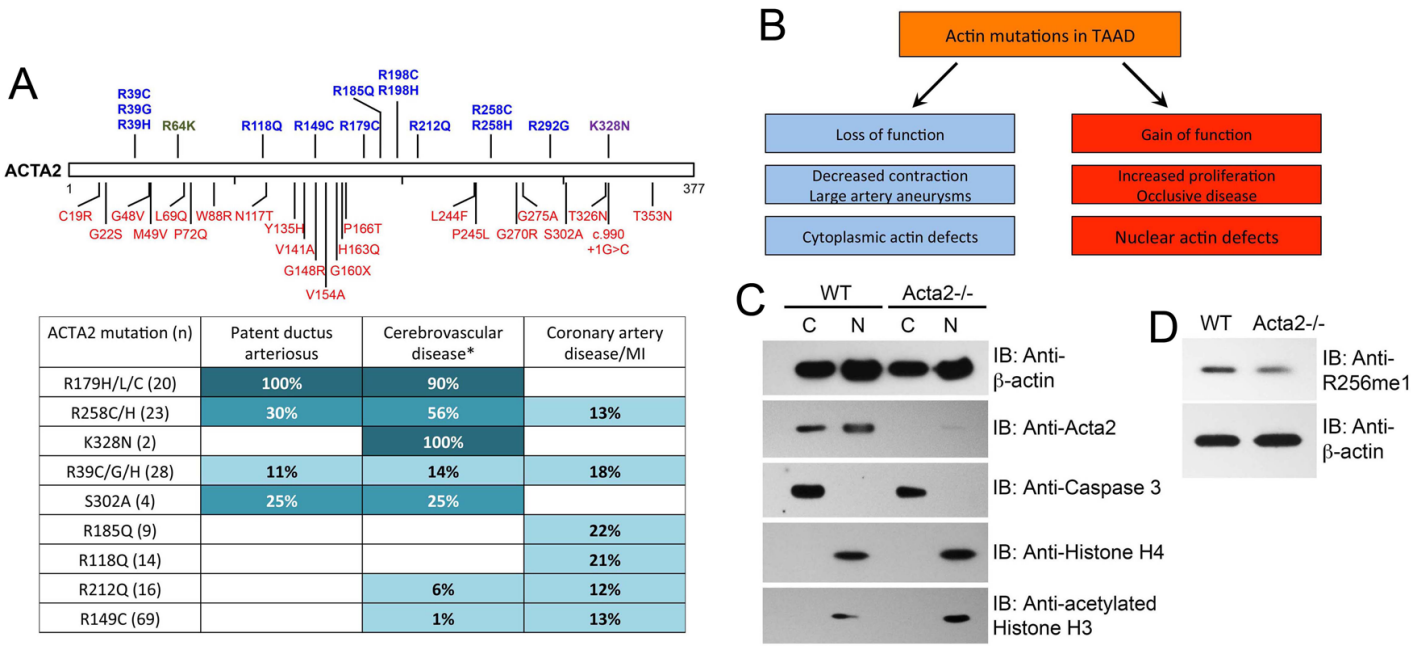

ACTA2 mutation (n)	Patent ductus arteriosus	Cerebrovascular disease*	Coronary artery disease/MI
R179H/L/C (20)	100%	90%	
R258C/H (23)	30%	56%	13%
K328N (2)		100%	
R39C/G/H (28)	11%	14%	18%
S302A (4)	25%	25%	
R185Q (9)			22%
R118Q (14)			21%
R212Q (16)		6%	12%
R149C (69)		1%	13%

Figure S4: TAAD causing mutants of *ACTA2*. Related to Figure 5. (A), Table showing TAAD causing *ACTA2* mutations and their respective phenotypes. (B), Model showing gain of function mutations in *ACTA2* that cause TAAD in human were explained by cytoplasmic actin defects, however those TAAD causing ACTA2 mutations that result in loss of function could be explained by the defects in the nuclear functions of actin. (C), Western blot analysis of cytoplasmic and nuclear fractions of WT and Acta2-/- smooth muscle cells from mice using antibodies as indicated. Actin (C4) was used for loading control, caspase3 was used for cytoplasmic fraction marker, histone H4 and acetylated Histone H3 were used as nuclear fraction markers. (D), Western blot analysis of nuclear fractions of WT and Acta2-/- smooth muscle cells from mice using antibodies as indicated. Actin (C4) was used for loading control.

Figure S5

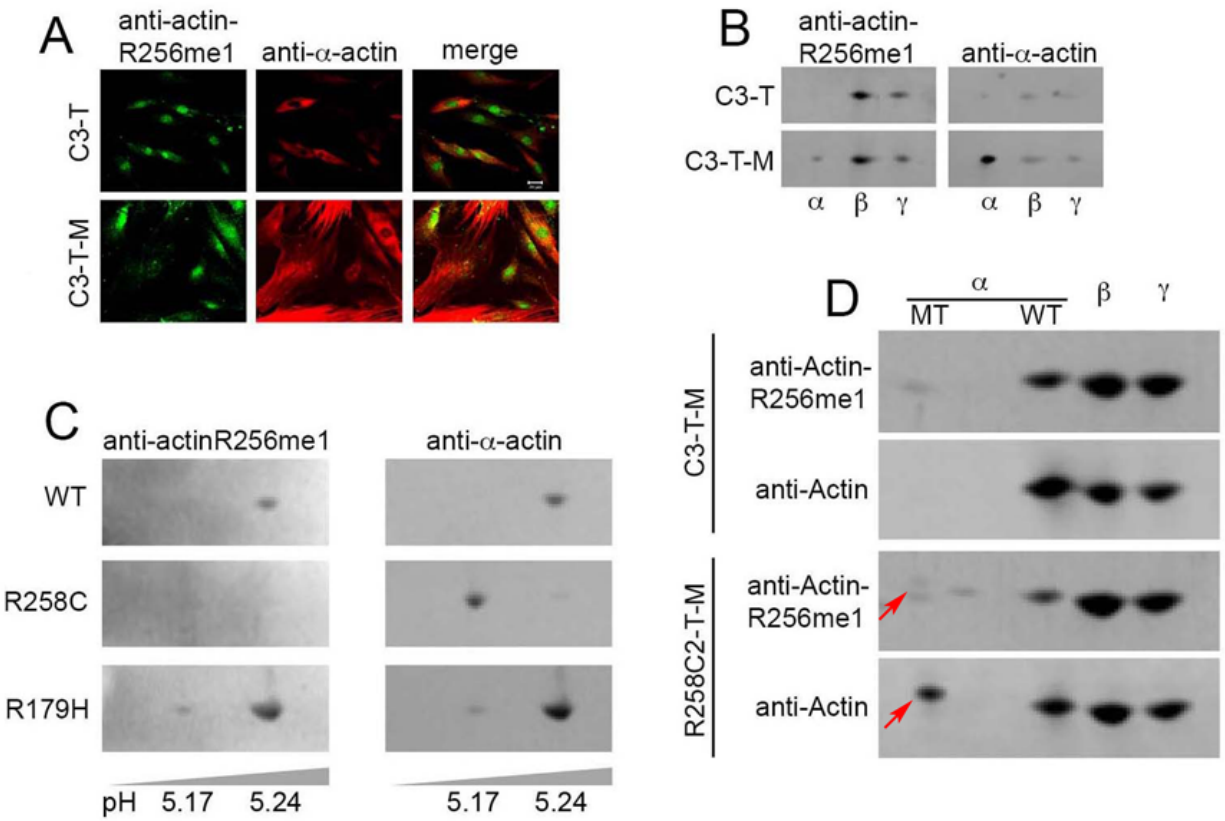

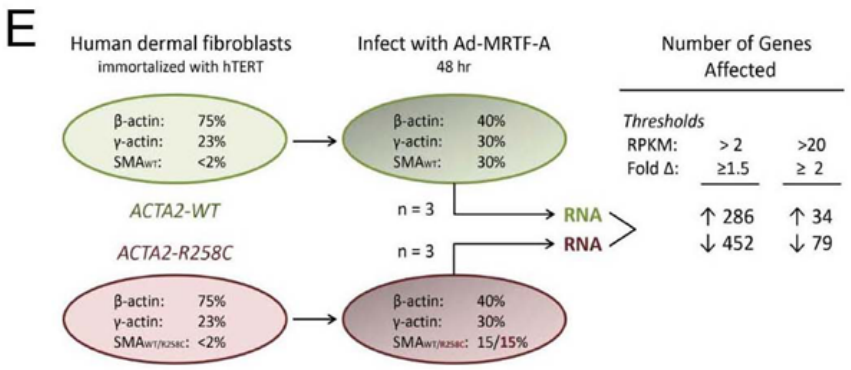

Ingenuity Canonical Pathways with p<0.0001			
PATHWAY RPKM >2, Fold Δ ≥1.5	**-log (p-value)**	**% Pathway Genes Affected**	**Number of Genes Up/Down: Total**
Interferon Signaling	6.39	26.5	0/9: 34
Hepatic Fibrosis/ Hepatic Stellate Cell Activation	5.65	9.9	8/12: 202
Death Receptor Signaling	4.11	12.0	2/9: 92
RPKM >20, Fold Δ ≥2			
Interferon Signaling	6.34	14.7	0/5: 34
Glutathione-mediated Detoxification	4.44	9.8	1/3: 41
Cell Cycle: G2/M DNA Damage Checkpoint Regulation	4.13	8.2	0/4: 49

Figure S5: Mutation of smooth muscle α-actin, ACTA2-R258C (R256C in yeast actin), abrogates methylation and affects mRNA expression profile in R258C TAAD patient fibroblasts. Related to Figure 5.

(A), Immunofluorescence images of fibroblast showing R258me1-actin staining in the nucleus. R258me1-actin is enriched in nuclei of human fibroblasts before (C3-T) and after (C3-T-M) induction of SM-α-actin. R258me1-actin, green; SM-α-actin, red; scale bar 20 μM. (B), Western blot analysis of 2D gel of nuclear fractions from patient derived fibroblast. Membrane was first probed with actin R256me1 antibodies (1:100), followed by SM-α-actin antibodies (1:10,000) after washing with TBST. Actin isoforms are labeled. (C), Western blot analysis of 2D gel of purified recombinant WT-, R258C- and R179H-SM-α-actin with calculated isoelectric points: WT=5.24, R258C=5.17 and R179H=5.23. Blots were probed with actin R256me1 antibodies (1:500) followed by SM-α-actin antibodies (1:20,000) after stripping. Protein loading: 0.8μg WT-SM-α-actin; 0.8μg R258C-SM-α-actin. 0.9μg R179H-sm-α-actin. (D), Western blot analysis of 2D gel actin isoforms from Ad-MRTF-A infected WT (C3-T-M) and R258C (R258C2-T-M) mutant (MT) fibroblasts. Membrane was first probed with actin R256me1 antibodies (1:100), followed by SM-α-actin antibodies (1:10,000) after stripping with TBST. Presented here is the representative blot of 3 experiments on independent cell preparations. (E), R258C mutation in ACTA2 affects the transcriptional profile of human dermal fibroblasts. Top Panel. Schematic of protocol of sample preparation for RNA-Seq. Lower Panel: Table of Ingenuity Canonical Pathways with $p<0.0001$ at both low (RPKM >2, Fold change (Δ) ≥1.5) and high (RPKM >20, Δ ≥2) stringency.

Figure S6

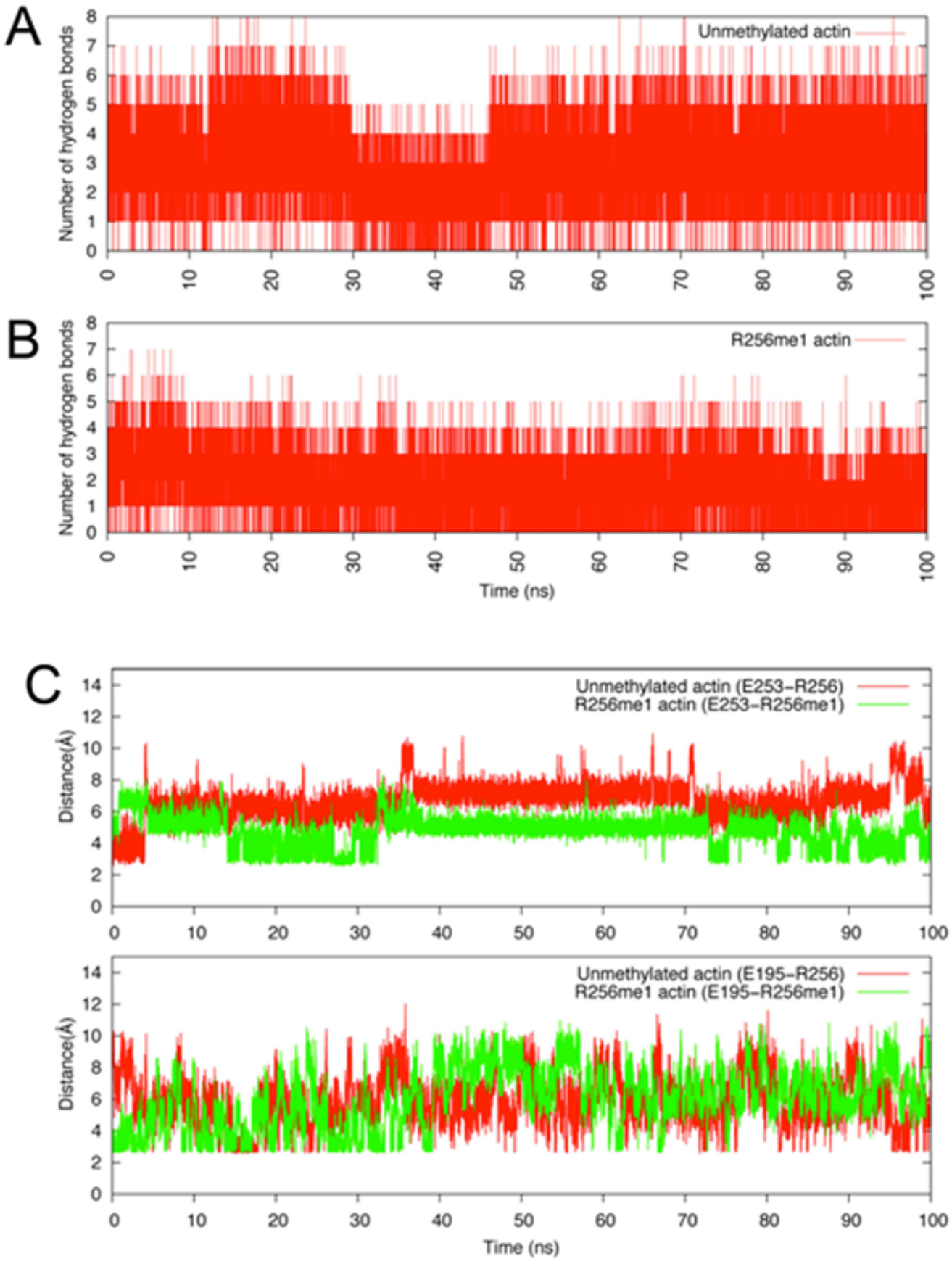
A
Unmethylated actin
Number of hydrogen bonds
B
R256me1 actin
Number of hydrogen bonds
Time (ns)
C
Unmethylated actin (E253–R256)
R256me1 actin (E253–R256me1)
Distance(Å)
Unmethylated actin (E195–R256)
R256me1 actin (E195–R256me1)
Distance(Å)
Time (ns)

Figure S6: MD Simulation analysis. Related to Figure 6. (A-B)**,** Presented here is the total number of inter-molecular hydrogen bond interactions between ATP; and (A), wild-type actin (unmethylated), and (B), methylated actin (actin R256me1). (C), Presented here is the distance between OE1 atom of E253 or E195 and NH2 of R256 monitored as a function of MD simulation time. Please also see Figure 6.